Supporting information

Fe-N-C Artificial Enzyme: Activation of Oxygen for Dehydrogenation and Monoxygenation of Organic Substrates under Mild Condition and Cancer Therapeutic Application

Fei He,[a] Li Mi,[a] Yanfei Shen,[a] Toshiyuki Mori,[b] Songqin Liu[a] and Yuanjian Zhang[a]*

[a]Jiangsu Engineering Laboratory of Smart Carbon-Rich Materials and Device, Jiangsu Province Hi-Tech Key Laboratory for Bio-Medical Research, School of Chemistry and Chemical Engineering, Medical School, Southeast University, Nanjing 211189, China

[b]Global Research Center for Environment and Energy Based on Nanomaterials Science (GREEN), National Institute for Materials Sciences (NIMS), 1-1 Namiki, Ibaraki, 305-0044, Japan

(*) Email: Yuanjian.Zhang@seu.edu.cn

Characterization. UV-Vis absorption spectroscopy was measured on an Agilent Cary 100 UV-Vis spectrophotometer (USA). HPLC analysis was performed on a Shimadzu LC-2010C system (Japan) equipped with a build-in UV-Vis detector and a Agilent ZOBAX NH_2 (5 μm, 250 × 4.6 mm) column (USA). Scanning electron microscopy (SEM) images of the samples were recorded by using a Zeiss Ultra Plus field emission scanning electron microscope (German) at an acceleration voltage of 10 kV. Transmission electron microscopy (TEM) was carried out on a JEOL 2100F (Japan) at an accelerating voltage of 200 kV. Raman spectra were measured on a Thermo DXR 532 Raman spectrometer (USA) with a laser excitation wavelength of 532 nm. X-Ray diffraction (XRD) was carried out on a Rigaku Smartlab 3 (Japan) X-ray diffractometer equipped with graphite monochromatic Cu Kα radiation (λ=1.54056Å). X-Ray Photoelectron Spectroscopy (XPS) experiments were performed in a Thermo Theta probe (USA) using monochromated Al Kα X-rays at hν 1486.6 eV. Peak positions were internally referenced to the C1s peak at 284.6 eV. Dissolved oxygen was measured by a Rex JPSJ-605 meter (China).

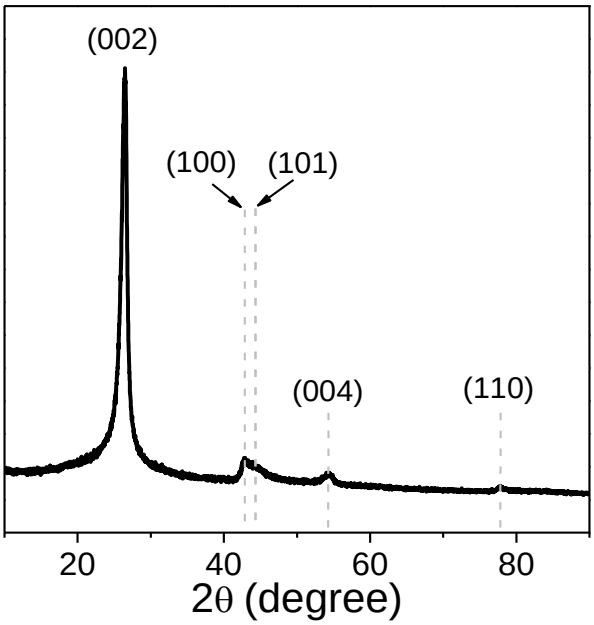

Figure S1 XRD pattern of Fe-N-C.

Fe-N-C comprised of graphitic carbon, as evidenced by the characteristic XRD peaks at ~26.2°, 42.6°, 44.4°, 54.3° and 77.8° corresponding to the (002), (100), (101), (004) and (110) diffractions, respectively. Few Fe-related clusters or nanoparticles were observed in XRD, agreeing well with the TEM result (Figure 1c and 1d) and suggesting a uniform distribution of Fe in Fe-N-C, most presumably in the Fe-N_x complexing manner.

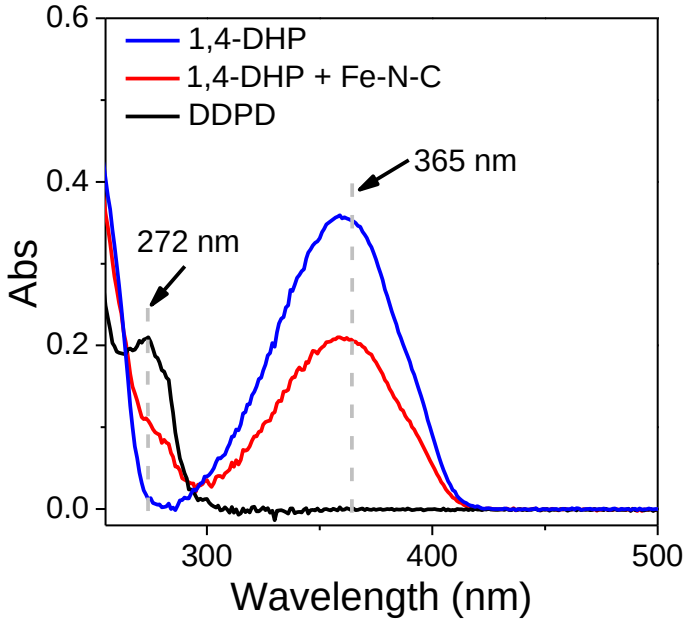

Figure S2 UV-vis spectra of 1, 4-DHP with and without Fe-N-C and diethyl 2,6-dimethyl-3,5-pyridine-dicarboxylate (DDPD).

1, 4-DHP showed a UV-vis absorbance peak at 365nm. After Fe-N-C catalyzed oxidation, a new absorption peak at 272 nm, typically ascribing to pyridine-based derives DDPD, was observed in the UV-vis spectrum of the product, an evident proof of the occurrence of the catalytic oxidative dehydrogenation reaction.

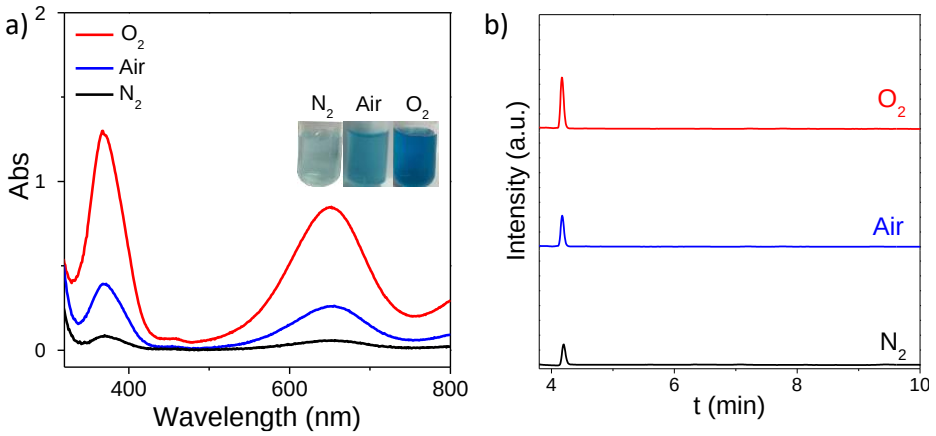

Figure S3 (a) UV-Vis spectra of Fe-N-C catalyzed TMB oxidation. TMB: 408 μM pH= 4.0 (b) HPLC chromatogram of Fe-N-C catalyzed 1, 4-DHP oxidation under N_2, O_2 and air-saturated solution. [1, 4-DHP]= 250 μM

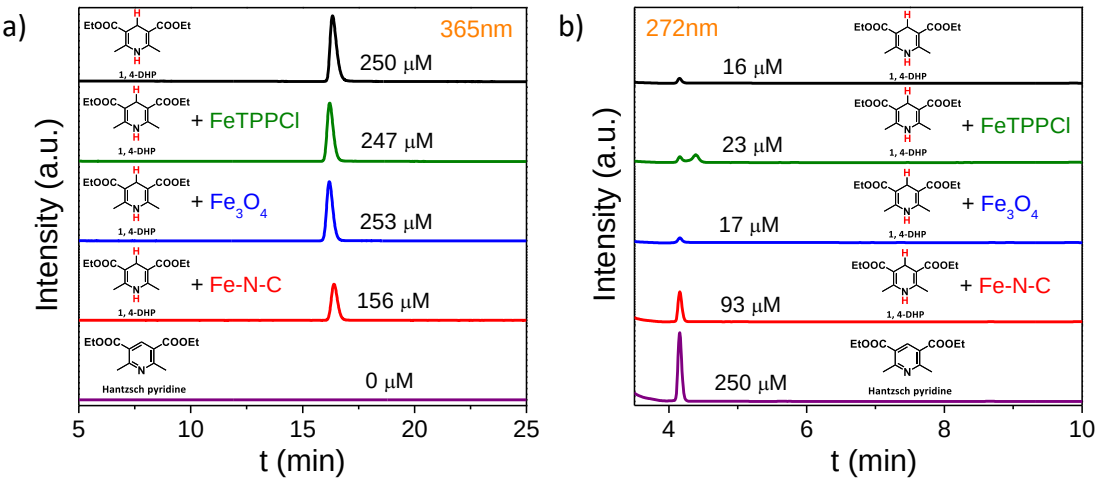

Figure S4 HPLC chromatograms of 1, 4-DHP (a) and the dehydrogenation product DDPD (b) of 1, 4-DHP catalyzed by various catalysts. Both of the concentration of 1, 4-DHP and DDPD were 250 μM.

The absorbance peaks of 1, 4-DHP and DDPD were 365 and 272nm, respectively (Figure S2). As shown in Figure S4a, adding FeTPPCl and nano-Fe_3O_4 into the 1,4-DHP solution would not decrease the intensity of peak at 16.3 min, indicating FeTPPCl and nano-Fe_3O_4 could not employ dioxygen to dehydrogenate 1,4-DHP in aqueous solutions under mild conditions. In contrast, the peak intensity of 1,4-DHP decreased when Fe-N-C was introduced into the 1,4-DHP solution (Figure S4a), and the single product peak was observed obviously at 4.2 min, which was attributed to DDPD (Figure S4b). These results demonstrated Fe-N-C could catalyze the dehydrogenation of 1,4-DHP with high selectivity by directly employing O_2 as oxidant.

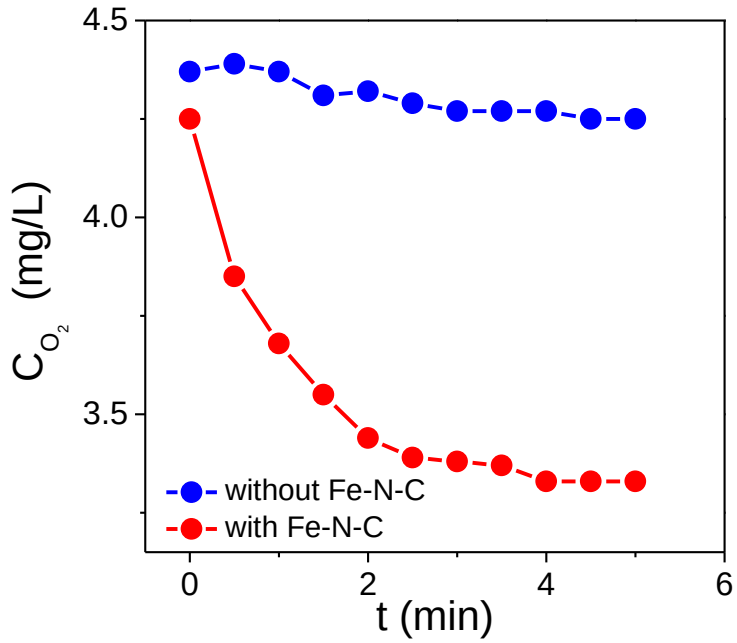

Figure S5 Measurement of O_2 concentration in air-saturated phosphate buffer solution (pH=7.4) with and without Fe-N-C catalyzed dehydrogenation of 1, 4-DHP.

As shown in Figure S5, without Fe-N-C, the O_2 concentration of solution nearly kept constant. After adding Fe-N-C, the O_2 concentration decreased rapidly, indicating Fe-N-C could dehydrogenate 1, 4-DHP by using dioxygen in aqueous solutions under mild condition.

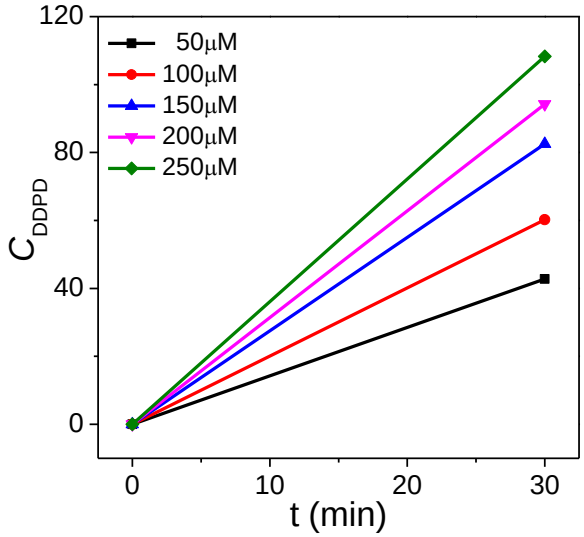

Figure S6 Oxidation of 1, 4-DHP catalyzed by Fe-N-C at different concentration.

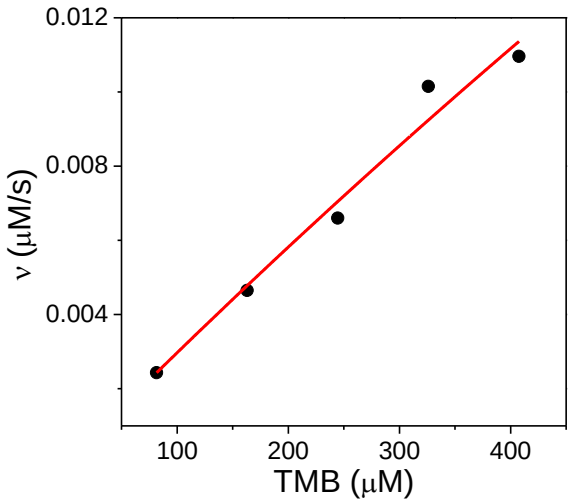

Figure S7 Kinetics for oxidase-like activity of Fe-N-C. [Fe-N-C]= 25 μg/mL, pH=3.6.

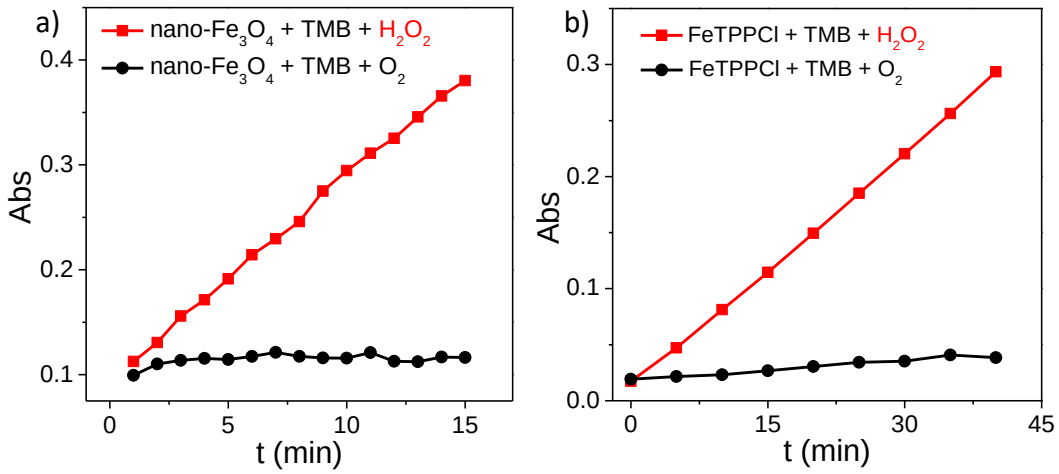

Figure S8 Time-dependent UV-Vis absorbance for oxidation of 3,3',5,5'-tetramethylbenzidine (TMB) at 652 nm catalyzed by nano-Fe_3O_4 (a) and FeTPPCl (b) in the presence of H_2O_2 and O_2.

As shown in Figure S8, both of nano-Fe_3O_4 and FeTPPCl could employ H_2O_2 to catalyze oxidation of TMB in HAc/NaAc buffer solution (pH=3.6), which agreed well with the reported result (ref: Gao L, Zhuang J, Nie L, Zhang J, Zhang Y, Gu N*, et al.* Intrinsic peroxidase-like activity of ferromagnetic nanoparticles. *Nat. Nanotechnol.* 2007, **2**, 577; Zhou Y, Huang X, Zhang W, Ji Y, Chen R, Xiong Y. Multi-branched gold nanoflower-embedded iron porphyrin for colorimetric immunosensor. *Biosens. Bioelectron.* 2017, **102**, 9). In contrast, they could not utilize O_2 to oxidize TMB. In this regard, nano-Fe_3O_4 and FeTPPCl could not act as biomimetic P450-like catalyst that directly use dioxygen.

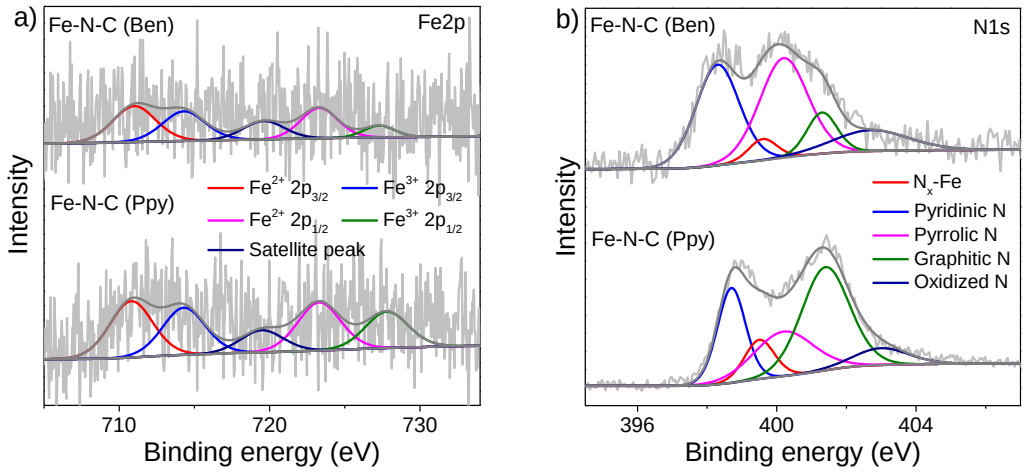

Figure S9 (a) Fe2p and (b) N1s XPS spectra of Fe-N-C (Ben) and Fe-N-C (Ppy).

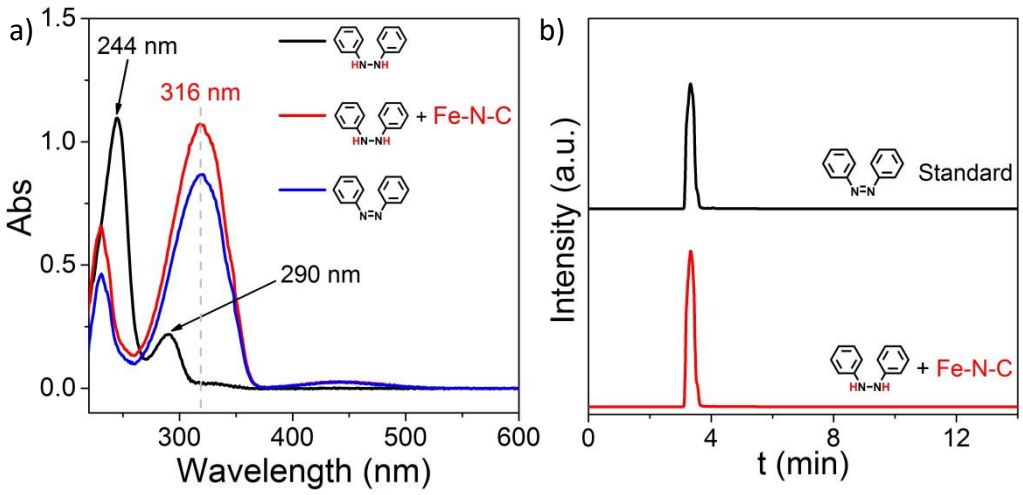

Figure S10 UV-vis spectra (a) and HPLC chromatogram (b) of diphenylhydrazine, azobenzene and diphenylhydrazine oxidation catalyzed by Fe-N-C.

Diphenylhydrazine showed two absorbance peaks at 244 and 290 nm when no Fe-N-C was introduced into air-saturated aqueous solution. However, such two peaks disappeared after adding Fe-N-C, and a new peak at 316 nm appeared, which was attributed the product of azobenzene. The similar result was also confirmed by HPLC, indicating Fe-N-C could dehydrogenate diphenylhydrazine by using dioxygen in aqueous solutions under mild conditions.

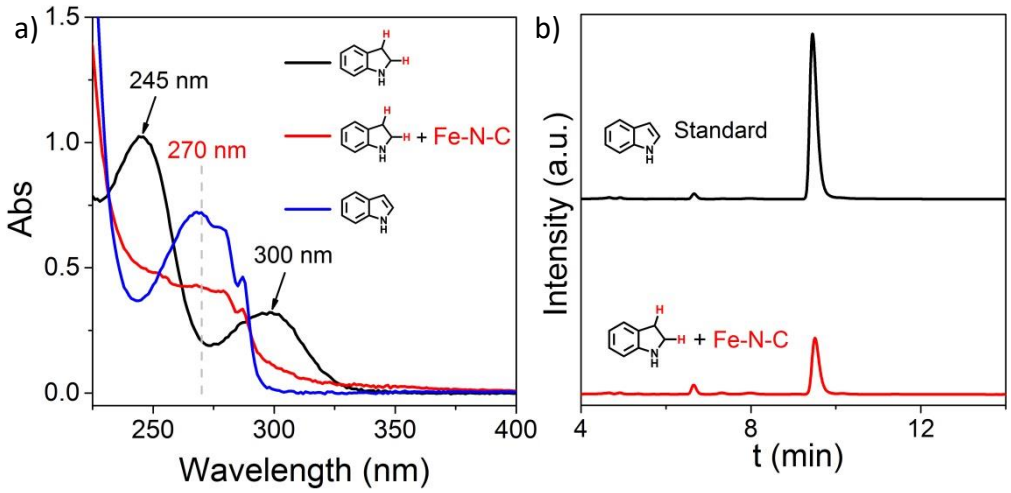

Figure S11 UV-vis spectra (a) and HPLC chromatogram (b) of indoline, indole and indoline oxidation catalyzed by Fe-N-C.

Indoline showed two absorbance peaks at 245 and 300 nm when no Fe-N-C was introduced into air-saturated aqueous solution. However, such two peaks disappeared after adding Fe-N-C, and a new peak at 270 nm appeared, which was attributed the product of indole. The similar result was also confirmed by HPLC, indicating Fe-N-C could dehydrogenate indole by using dioxygen in aqueous solutions under mild conditions.

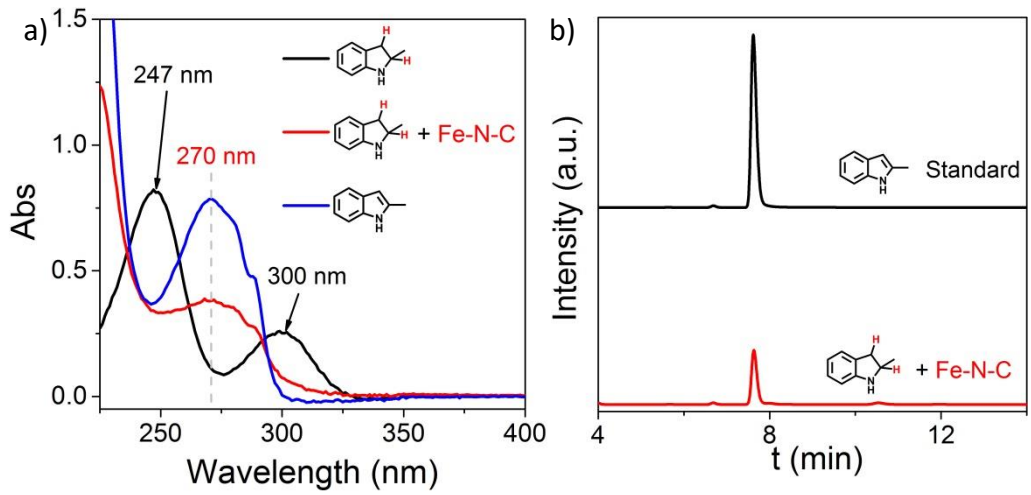

Figure S12 UV-vis spectra (a) and HPLC chromatogram (b) of 2-methylindoline, 2-methylindole and 2-methylindoline oxidation catalyzed by Fe-N-C.

2-Methylindoline showed two absorbance peaks at 247 and 300 nm when no Fe-N-C was introduced into air-saturated aqueous solution. However, such two peaks disappeared after adding Fe-N-C, and a new peak at 270 nm appeared, which was attributed the product of 2-methylindole. The similar result was also confirmed by HPLC, indicating Fe-N-C could dehydrogenate 2-methylindoline by using dioxygen in aqueous solutions under mild conditions.

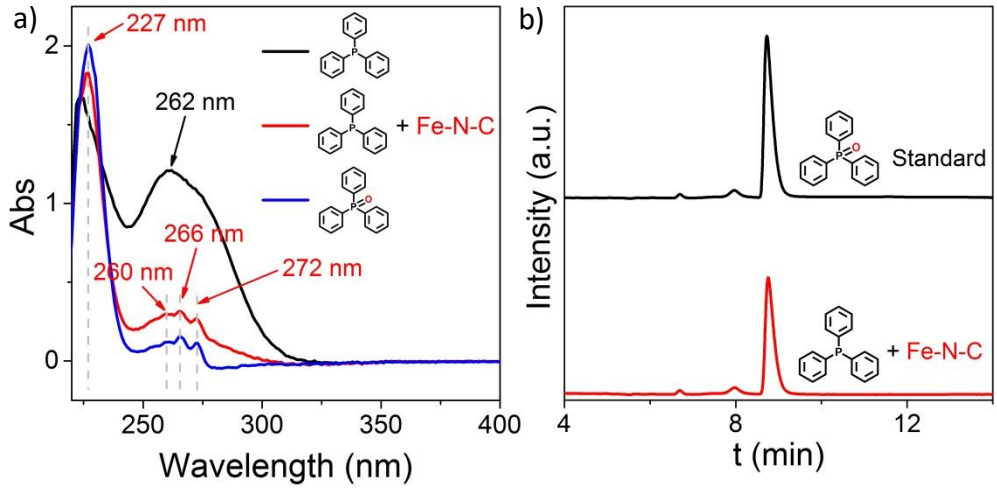

Figure S13 UV-vis spectra (a) and HPLC chromatogram (b) of triphenylphosphine, triphenylphosphine oxide and triphenylphosphine oxidation catalyzed by Fe-N-C.

Triphenylphosphine showed an absorbance peak at 262 nm when no Fe-N-C was introduced into air-saturated aqueous solution. However, such peak disappeared after adding Fe-N-C, and four new peaks at 227, 260, 266 and 272 nm appeared, which were attributed the product of triphenylphosphine oxide. The similar result was also confirmed by HPLC, indicating Fe-N-C could monoxygenate triphenylphosphine by using dioxygen in aqueous solutions under mild conditions.

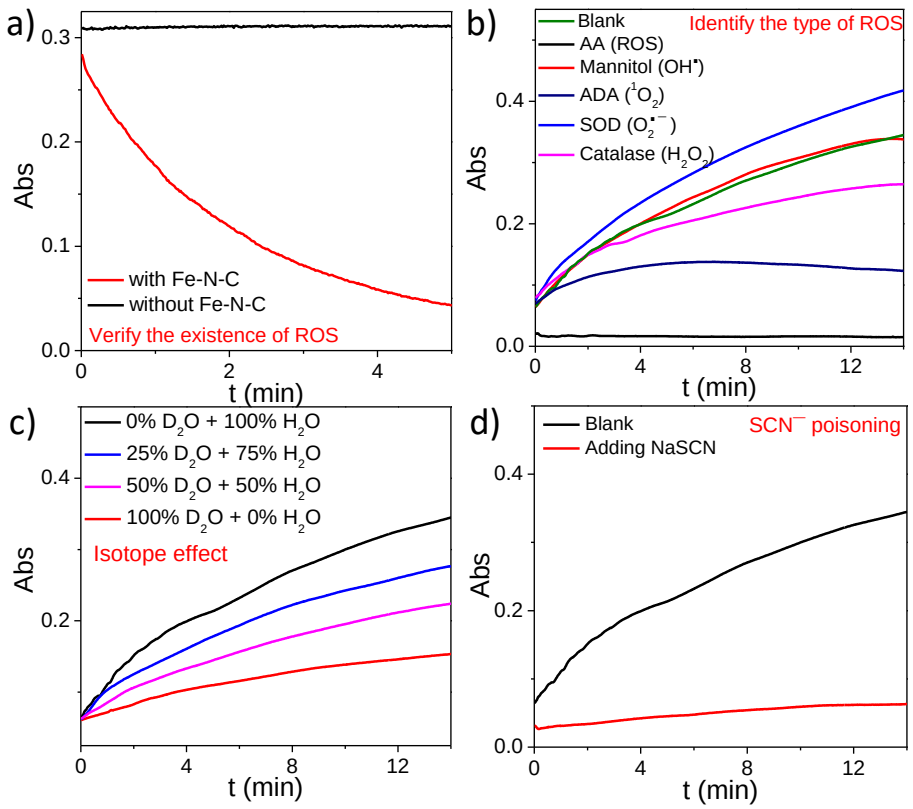

Figure S14 Time-dependent UV-Vis absorbance and possible mechanism of dioxygen activation on Fe-N-C artificial enzyme. (a) Oxidation of ascorbic acid (AA) at 245 nm in the absence or presence of Fe-N-C. (b) Oxidation of 3,3',5,5'-tetramethylbenzidine (TMB) at 652 nm in the absence or presence of $^1O_2$, $O_2^{\bullet-}$, $OH^{\bullet}$ and H_2O_2 scavengers. (c) Oxidation of TMB at 652 nm with different content of D_2O. (d) Oxidation of TMB at 652 nm in the absence or presence NaSCN.

Table S1 The proportion of different N species in catalysts from XPS

Catalyst	pyridinic N	N_x-Fe	pyrrolic N	graphitic N	oxidized N
Fe-N-C	27.4%	9.1%	22.4%	32.6%	8.6%
Fe-N-C (Ben)	34.6%	4.9%	38.0%	10.0%	12.5%
Fe-N-C (Ppy)	21.6%	9.6%	21.2%	40.0%	7.6%

Table S2 Comparison of the kinetic parameters of different artificial enzymes for dehydrogenation of 1, 4-DHP by direct using oxygen in aqueous solution.

Entry	Catalyst	K_{cat} min^{-1}	K_m mM	V_{max} mM min^{-1}	K_{cat}/K_m mM^{-1} min^{-1}
1	FeTPPCl[a]	N.D.	N.D.	N.D.	N.D.
2	nano-Fe_3O_4[a] artificial enzyme[a]	N.D.	N.D.	N.D.	N.D.
3	Fe-N-C artificial enzyme[a]	1.24	0.264	7.89×10^{-3}	4.70
4	Fe-N-C (Ben) artificial enzyme[a]	0.630	0.228	5.51×10^{-3}	2.76
5	Fe-N-C (Ppy) artificial enzyme[a]	0.591	0.176	5.81×10^{-3}	3.36
6	Fe-N-C artificial enzyme[b]	/	4.58	8.35×10^{-3}	/
7	N-PCNSs-3[c]	/	0.084	2.52×10^{-4}	/

[a] Catalytic oxidation of 1,4-DHP. [b] Catalytic oxidation of TMB. [c] The value was obtained from Nat. Commun., 2018, 9, 1440.

Table S3 Kinetic parameters of P450 enzymes for dehydrogenation of N-heterocycles by direct using oxygen in aqueous solution (adapted from Sun H, Ehlhardt WJ, Kulanthaivel P, Lanza DL, Reilly CA, Yost GS. Dehydrogenation of indoline by cytochrome P450 enzymes: a novel "aromatase" process. *J. Pharmacol. Exp. Ther.* 2007, **322**, 843).

Entry	Catalyst	K_{cat}	K_m	V_{max}	K_{cat}/K_m
		min^{-1}	mM	mM min^{-1}	mM^{-1} min^{-1}
1	CYP2E1	0.36	0.166	-	2.2
2	CYP2B6	0.98	0.106	-	9.2

Table S4 Comparison of the reported catalysts and this work regarding the terminal oxidant, additional mediators, and other complementary conditions

	Catalyst	**Terminal oxidant**	**Additional Mediators or complementary conditions**	**Remark**
Nat. Nanotechnol., **2007**, 2, 577	Fe_3O_4 nanoparticles	H_2O_2	Only work in Acidic aqueous solution	b, c
Adv. Mater. **2010**, 22, 2206-2210	Graphene oxide	H_2O_2	Only work in Acidic aqueous solution	b, c
Angew. Chem. Int. Ed., **2012**, 51, 3822	Graphene-porphyrin	H_2O_2	No	b, d
J. Am. Chem. Soc., **1984**, 106, 6668	(Porphyrinato)manganese	NaClO	No	a, d
J. Am. Chem. Soc., **2003**, 125, 14674	Iron porphyrin	m-CPBA	No	a, d
J. Am. Chem. Soc., **2016**, 138, 499	Mn-porphyrins	PhIO	No	a, d
J. Am. Chem. Soc., **2012**, 134, 8014	Mn complex	O_2	Light	a, d
Angew. Chem. Int. Ed. **2014**, 53, 8824.	CuCl	O_2	TEMPO	a, c
Angew. Chem. Int. Ed. **2009**, 48, 2308	Polymer-coated Cerium oxide nanoparticles	O_2	Only work in Acidic aqueous solution	b, c
Nat. Chem., **2018**, 10, 200	$CoCl_2$	O_2	PhI /Aldehydes	a, c
-	Cytochrome P450 (CYP)	O_2	Only work in mild condition	a, c, d
This work	**Fe-N-C**	**O_2**	**No**	b, c, d

[a] Homogeneous, [b] Heterogeneous, [c] Dehydrogenation, [d] Monoxygenation